

This paper was presented at a colloquium entitled “Neuroimaging of Human Brain Function,” organized by Michael Posner and Marcus E. Raichle, held May 29–31, 1997, sponsored by the National Academy of Sciences at the Arnold and Mabel Beckman Center in Irvine, CA.

The representation of the ipsilateral visual field in human cerebral cortex

ROGER B. H. TOOTELL*, JANINE D. MENDOLA, NOUCHINE K. HADJIKHANI, ARTHUR K. LIU, AND ANDERS M. DALE

Nuclear Magnetic Resonance Center, Massachusetts General Hospital, 149 13th Street, Charlestown, MA 02129

ABSTRACT Previous studies of cortical retinotopy focused on influences from the contralateral visual field, because ascending inputs to cortex are known to be crossed. Here, functional magnetic resonance imaging was used to demonstrate and analyze an ipsilateral representation in human visual cortex. Moving stimuli, in a range of ipsilateral visual field locations, revealed activity: (i) along the vertical meridian in retinotopic (presumably lower-tier) areas; and (ii) in two large branches anterior to that, in presumptive higher-tier areas. One branch shares the anterior vertical meridian representation in human V3A, extending superiorly toward parietal cortex. The second branch runs antero-posteriorly along lateral visual cortex, overlying motion-selective area MT. Ipsilateral stimuli sparing the region around the vertical meridian representation also produced signal reductions (perhaps reflecting neural inhibition) in areas showing contralaterally driven retinotopy. Systematic sampling across a range of ipsilateral visual field extents revealed significant increases in ipsilateral activation in V3A and V4v, compared with immediately posterior areas V3 and VP. Finally, comparisons between ipsilateral stimuli of different types but equal retinotopic extent showed clear stimulus specificity, consistent with earlier suggestions of a functional segregation of motion vs. form processing in parietal vs. temporal cortex, respectively.

In primates and other mammals, it is well accepted that visual input to each cerebral cortical hemisphere comes largely from the contralateral visual hemifield. For example, in macaque monkeys, input to primary visual cortex (V1) appears completely crossed, with little (1) or no (2) measurable activation from the ipsilateral visual field.

However, in progressively higher-tier cortical areas of macaque, neurons have correspondingly larger receptive fields, including increasing input from the visual field on the same (ipsilateral) side of the brain. In lower-tier visual areas, this ipsilateral input occurs primarily near the retinotopic representation of the vertical meridian. The vertical meridian is the “seam” in the brain along which the representations of left and right hemifields are united, via connections across the corpus callosum. In higher-tier areas, receptive fields become so large and bilateral that retinotopy is difficult or impossible to demonstrate. Nevertheless, it is presumed that the same relationship of callosal terminations along a coarsely defined vertical meridian representation is preserved (3–8).

Even in higher-tier cortical regions where retinotopy cannot be resolved, neurons vary in the extent of their ipsilateral representation. For instance, neurons in macaque area MST have receptive fields that are larger and extend further into the

ipsilateral visual field, compared with receptive fields in immediately adjacent area MT (9–12). Other examples include areas LIP (13) and V4 (14), which show very little excitatory hemispheric overlap, whereas cells in other regions such as inferotemporal cortex show a great deal of ipsilateral activation (15). Such electrophysiological variations in the ipsilateral activation may reflect corresponding variations in the density of callosal inputs within the same cortical regions (e.g., ref. 16).

It is likely that a similar representation of the ipsilateral visual field exists in human visual cortex (17–19). However, maps of ipsilateral activity have not been imaged previously in any species, to our knowledge.

If such maps could be obtained from human cortex, this information would clarify the relative independence of stimuli presented to left and right hemispheres in previous psychophysical comparisons of callosally sectioned (e.g., refs. 20 and 21) and normal subjects. Such ipsilateral maps also should help to distinguish between different higher-order areas in human cortex, where functional mapping distinctions are still somewhat murky (22, 23). It also should be possible to relate such maps of ipsilateral activity to the anatomical patterns of callosal degeneration, mapped in previous studies of human visual cortex (17–19).

Mapping the Ipsilateral Retinotopy in Human Visual Cortex

We mapped the ipsilateral representation throughout human visual cortex by using functional magnetic resonance imaging (fMRI). Twelve subjects were scanned (85 scans, 2,048 images/scan) while viewing ipsilateral visual stimuli in a 1.5-T General Electric scanner retrofitted with echo-planar imaging (ANMR), by using a bilateral quadrature surface coil covering visual cortex. Detailed procedures are described elsewhere (24). In these and other subjects, cortical areas also were mapped by presenting a battery of additional bilateral stimuli, previously used to define human cortical areas V1, V2, V3, VP, V3A, and V4v (126 scans) (23–31) and MT (185 scans) (23, 24, 28, 32–36). For optimal views of the cortical topography, data were analyzed and displayed by using cortical unfolding/flattening procedures (23, 24, 29, 35, 37). These procedures are conceptually similar to flattening approaches described by other groups (e.g., refs. 30, 31, and 38).

A representative ipsilateral stimulus is shown in Fig. 14. Moving black-and-white rings were presented within a retinotopically fixed sector, avoiding a central circular region (0.5°

Abbreviations: fMRI, functional magnetic resonance imaging; MR, magnetic resonance.

*To whom reprint requests should be addressed. e-mail: tootell@nmr.mgh.harvard.edu.

radius) containing the fixation point. The stimulus in Fig. 1*A* was displaced by 20° of polar angle from the vertical meridian; other stimuli (outlined in Fig. 1*B*) were displaced by either 0°, 5°, 10°, or 40°. Stimuli were presented either to the left or right hemifield within a given scan, always in alternation (16-sec epochs) with a uniform gray control stimulus including a central fixation point. Subjects were instructed to stare continuously at the fixation point during fMRI acquisition.

The stimulus displacement from the vertical meridian increased with eccentricity, to approximate the well-known and systematic decreases in cortical magnification factor with eccentricity. The rationale for this stimulus configuration was as follows. Because cortical receptive field size generally increases as cortical magnification decreases within a cortical area, a thin vertical line displaced from the vertical meridian would be expected to stimulate a smaller range of cortical polar angles at a large eccentricity than at a small eccentricity. To overcome this bias, for each stimulus, the edge of the occluding aperture was moved further away from the vertical meridian with increasing eccentricity. The goal was to shift the representation of the aperture's medial borders roughly as a line across cortex, approximately equal in cortical distance from vertical meridian representations, irrespective of stimulus eccentricity. The topography of the retinotopy in the contralateral hemisphere (see below) suggest that the polar coordinate stimuli used here approximately achieved this result.

Consistent with our basic hypothesis, such stimuli produced significant activation in the ipsilateral hemisphere. Fig. 1*C–G* shows the typical pattern in one subject, produced by the stimulus in Fig. 1*A*. The ipsilateral activation produced by these stimuli has a distinct topography, consisting of two broad branches (see Fig. 1 and below). One branch extends superiorly toward inferior parietal cortex, and the other one runs antero-posteriorly along the inferior lateral surface. Finding two distinctive branches of ipsilateral activation was not obviously predicted by the anatomical topography of callosal connections in previous animal experiments (3–8).

In most cortical regions, the amplitude of the ipsilateral magnetic resonance (MR) increase was not as high as that in the contralateral hemisphere; this finding is consistent with the generality of crossed visual input. In fact, in cortical regions showing significant contralateral retinotopy (e.g., areas V1, V2, and V3), there were consistent, significant decreases (blue through white) in response (relative to the control stimulus) during presentation of our ipsilateral visual field stimuli. This unusual finding does not appear to be because of “blood stealing” in the fMRI signals, at least in any simple way. However, the results are consistent with existing single-unit electrophysiology in animals demonstrating response inhibition by ipsilateral stimuli. In macaque area V4, at least, it has been reported that inhibitory ipsilateral influences extend much further into the ipsilateral visual field, compared with excitatory influences (14).

Contralateral Retinotopy of “Ipsilateral” Stimuli

In the contralateral (control) hemisphere, these stimuli produced a pattern of activation predictable from the shape of the stimulus relative to previously described retinotopic maps in areas V1, V2, V3, VP, V3A, and V4v. For example, Fig. 2*A* shows a map of the contralateral retinotopy in one subject, and Fig. 2*B* shows the contralateral response to our most restricted (40°) stimulus (see Fig. 1*B*), in the same subject. This unilateral stimulus activates the cortical representations of the contralateral horizontal meridian, but spares the representation of the vertical meridian and the foveal representation—exactly as predicted by the stimulus geometry. These control results confirmed the appropriateness of our polar coordinate stimuli, the fixation stability, and our understanding of the contralateral retinotopy.

Relationship of Ipsilateral and Contralateral Retinotopy

Further analysis reveals that the ipsilateral activation is systematically related to other topographical features in the visual cortical map. For instance, the ipsilateral activation produced by the mid-range (20°) stimulus appeared to be concentrated immediately anterior to those areas showing classical (contralateral) retinotopy (e.g., V1, V2, V3, VP, V3A, and V4v). To test this idea directly, we compared the contralateral and ipsilateral representations in the same subjects, in the same hemispheres. Fig. 3 shows such a comparison, produced by stimuli in left and right visual hemifields (activated in different scans). It suggests that the ipsilateral representation indeed “begins” approximately where the contralateral retinotopy “ends.” Although the thresholds in such a comparison are not directly comparable, this same contralateral-to-ipsilateral retinotopic transition is apparent even when other thresholds and visual field extents are chosen (see Fig. 2 and below).

When using this same stimulus, the superior branch of ipsilateral activity borders the anterior portion of V3A, which is the most anterior and most coarsely retinotopic vertical meridian representation revealed by our current tests of contralateral retinotopy (see Fig. 3). That branch then continues superiorly with significant activation across the anterior segment of the transverse occipital sulcus, continuing anterior to and past the superior terminus of the parieto-occipital sulcus. The inferior branch of activity always begins near the foveal representation of V3/VP, extends somewhat inferiorly, and then somewhat superiorly through and beyond the motion-selective area MT (see Figs. 1, 3, and 4).

Range of Ipsilateral Influence

The above experiments reveal only a single “snapshot” of the ipsilateral representation. However, it is known that ipsilateral influence actually extends continuously but nonuniformly into different cortical regions, dependent on both cortical area boundaries and the retinotopy (if any) within each area (3–8, 16).

This complex spatial relationship was revealed by presenting the full set of ipsilateral stimuli (see Fig. 1*B*), within the same hemisphere (e.g., Fig. 4). Retinotopic cortical visual areas also were labeled as described elsewhere (23–31). The stimuli closest to the vertical meridian produced thin strips of activation extending along the representations of the vertical meridian, especially along the borders between V1 and V2 (see Fig. 4*C* and *D*). The appearance of activation along the vertical meridians of the ipsilateral hemisphere coincides with the complete filling-in of activation in the classic retinotopic areas of the contralateral hemisphere.

These tests also reveal differences in the overall extent of ipsilateral influence between different cortical areas. The most anterior retinotopic areas (V3A and V4v) show distinctively greater interhemispheric activation compared with immediately adjacent areas V3 and VP, across a considerable range of stimulus extents (see Fig. 4*B–D*). Although the ipsilateral architecture has not been imaged previously, these results are generally consistent with: (i) the retinotopy of these areas in humans (e.g., refs. 23–31) and macaques (e.g., ref. 39), (ii) related differences in receptive field sizes among areas in macaque (40) and human (24) cortex, and (iii) anatomical studies of callosal (interhemispheric) connections in animals (3–8, 16).

Control Stimulation Using Different Ipsilateral Stimuli

The two-branched topography revealed above is not predictable from the anatomical topography of callosal connections in macaques (3–8, 16) or humans (17–19). Of course, the topography of callosal connections is incompletely known in hu-

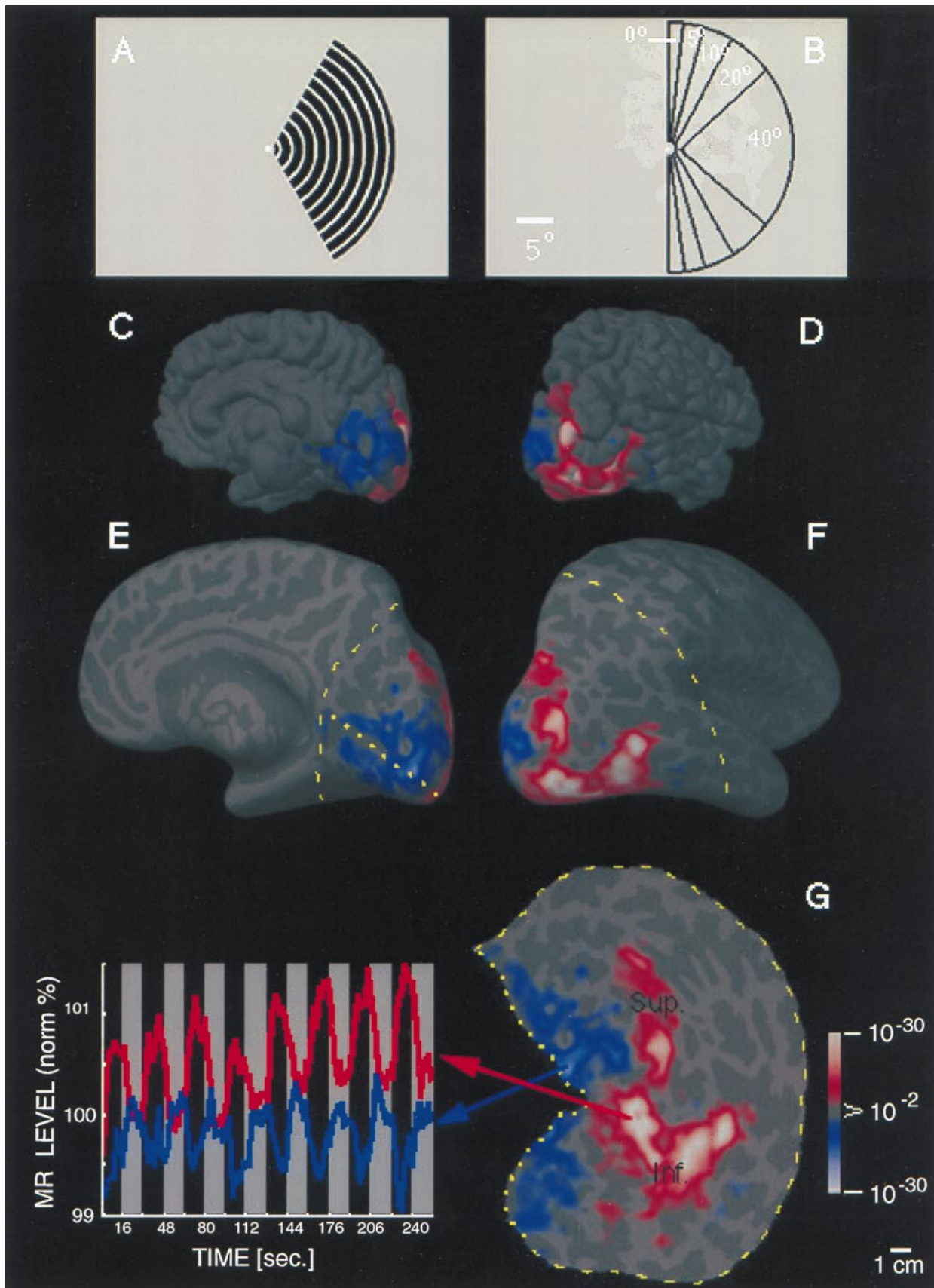


FIG. 1. Unilateral stimuli used in these experiments (*A* and *B*) and the topography of MR activity produced by one of these stimuli in the ipsilateral hemisphere (*C-G*). (*A*) A representative stimulus: a moving ($7^\circ/\text{sec}$), rectangular wave radial grating (0.5 cycles/degree, duty cycle = 0.2), confined to a fixed sector on either the right (as in *A*) or left side of a fixation point. (*B*) A diagram of the full range of sector sizes used: in different scans, stimuli spared the vertical meridian by either 0° , 5° , 10° , 20° , or 40° of polar angle. The stimulus in *A* spares the vertical meridian by 20° of polar angle. Calibration bar = 5° of visual angle. (*C-G*) Cortical activity produced in a representative ipsilateral hemisphere (subject AL) by the stimulus in *A*. Activity is shown in different views, including the normal, folded cortex (*C* and *D*), and in an "inflated" cortical format (*E*

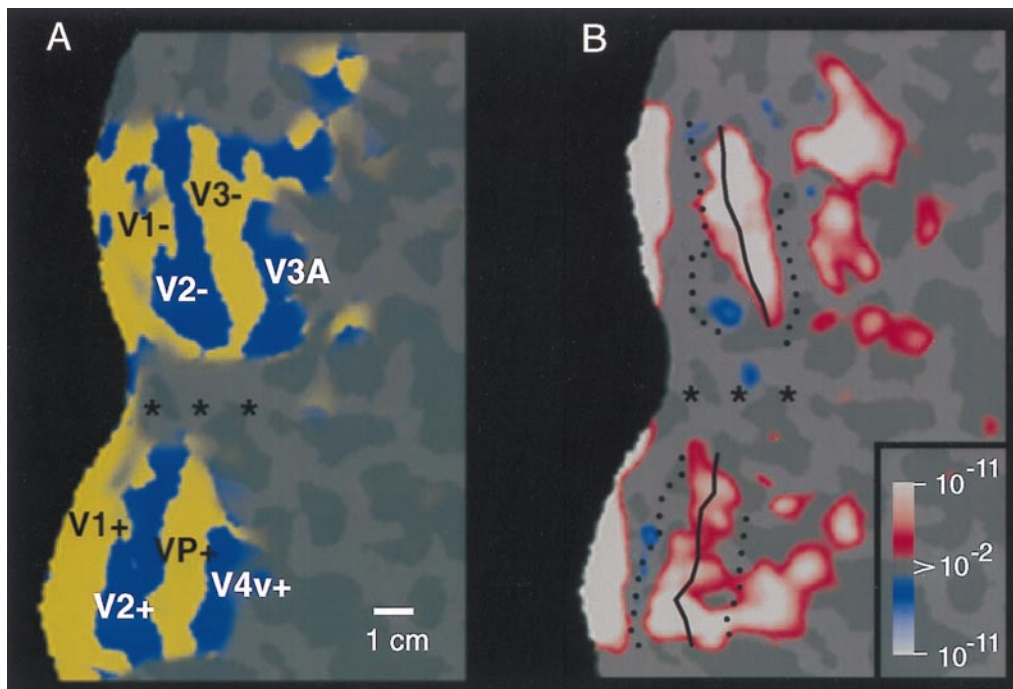


FIG. 2. Retinotopic specificity of one of our unilateral stimuli in the contralateral (control) hemisphere. (A) Area boundaries based on the contralateral retinotopic map in one hemisphere (subject BK), produced by “thin” versions of bilateral, phase-encoded stimuli described earlier (24). (B) The effect of one of the present stimuli, avoiding the vertical meridian by 40° , in the same (contralateral) hemisphere of that subject, acquired during a different scan. As one would predict from the retinotopic map and from the present stimulus geometry (assuming stable fixation), the present stimulus produces robust activation within much of areas V1, V2, V3, VP, V3A, and V4v, including the representation of the contralateral horizontal meridian representations (solid lines). Activity also is concentrated toward the left border of the flattened map, which also coincides with a horizontal meridian representation in the midline of primary visual cortex. However, little or no activation was produced along the representation of the vertical meridia (dashed lines), nor along the foveal representation (*). These features are consistent with the geometry of the contralateral stimulus, which also spared the vertical meridian and foveal representation, but included the horizontal meridian region. These results also confirmed the stability of fixation during the experiment. The other stimuli in this set, which encroached progressively closer to the vertical meridian, produced correspondingly more “filling in” of the vertical meridian representations; this finding is also consistent with the contralateral retinotopy (23–31). The pseudocolor activity representation is similar to that in Fig. 1. Increased MR signals in phase with grating presentation range from a display threshold of $P > 0.01$ (red) to a maximum of $P > 10^{-11}$ (white, surrounded by red). Regions of decreased MR signal level during grating presentation are rare in this hemisphere, but coded with a symmetrical color scale, from $P > 0.01$ (blue) to a minimum of $P > 10^{-11}$ (white, surrounded by blue). This data and data in subsequent figures are based on single scans (2,048 images), so maximal significance levels are correspondingly lower than those in Fig. 1. The location of sulci and gyri in the normal, folded cortical state are represented here in dark and light gray, respectively. The calibration bar represents 1 cm, without distortion correction; the distortion correction varies locally in the flattened maps but it typically averages $\pm 15\%$.

mans, and the anatomical and activity-based maps certainly have not been compared from the same human subjects.

Such a discrepancy could arise if our stimulus activated only a (dual branched) subset of those neurons (i.e., those responding to moving gratings) that also receive prominent callosal connections.

To test this idea, we presented a stimulus (naturalistic images) that was quite different from the moving gratings, but confined within the same ipsilateral apertures described in Fig. 1B. Although such naturalistic stimuli are impossible to specify in terms of linear systems analysis, they did satisfy our major goal: the naturalistic stimuli differed from our grating stimuli

and F) that shows activity normally hidden in cortical sulci. C and E are taken from a posterior-medial viewpoint, and D and F are taken from a posterior-lateral viewpoint. The ipsilateral activation and anatomical topography is more fully revealed in flattened cortical format (G), including posterior (visual) cortex. The arbitrary cut lines in the cortical surface are indicated by yellow lines (E–G: dotted = cut along the calcarine fissure; dashed = cut along the lateral surface). The pseudocolor scale bar indicates the statistical significance of the fMRI activity, based on an f-test. Increased MR signals in phase with grating presentation (i.e., conventional fMRI activity) range from a display threshold of $P > 0.01$ (red) to a maximum of $P > 10^{-30}$ (white, surrounded by red). Regions of decreased MR signal during grating presentation are coded with an inverted color scale, from $P > 0.01$ (blue) to $P > 10^{-30}$ (white, surrounded by blue). Maximum significance levels are relatively high partly because the data represents an average of eight identical scans (16,384 images total). The scale bar represents 1 cm (uncorrected for distortion) in the flattened image (G), 8 mm (E and F), and 6.7 mm (C and D). Although no stimulus appeared in the visual hemifield contralateral to this hemisphere at any time, there was significant positive fMRI activity (coded in red through white) in a bifurcating pattern on the lateral surface of the ipsilateral hemisphere (D, F, and G). From a common origin just lateral to the posterior pole, the superior branch (sup.) extends toward the superior terminus of the parieto-occipital fissure, and the inferior branch (inf.) runs antero-posteriorly along the inferior lateral surface. The ipsilateral stimulus also produces weaker, but statistically significant, decreases in MR level (blue through white) in the medial bank, where V1, V2, and other retinotopically specific areas are known to be located (refs. 23–31; see also Figs. 3 and 4). In corresponding regions of the contralateral hemisphere (see Fig. 2B), this unilateral stimulus produces robust increases in cortical activity, consistent with the known contralateral retinotopy. These activity maps were clarified by displaying the time course of MR changes from two regions of interest in this hemisphere. In the graph (Lower Left), the interhemispheric stimuli were presented during 16-sec epochs (black stripes), separated by epochs of stimulation with a uniform gray field (gray stripes). One time course is taken from the region showing the bifurcating MR-positive (red-white) responses during presentation of the interhemispheric stimuli (region indicated with red arrow). The other time course is taken from those regions (primarily in the medial bank) that show MR-negative changes (blue-white, indicated by blue arrow) during presentation of the interhemispheric stimuli, relative to intervening, uniform gray control stimuli.

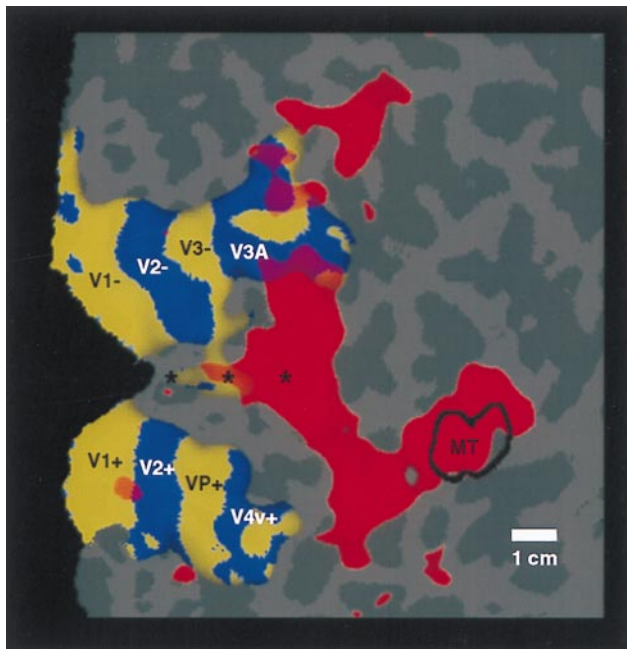


FIG. 3. Topographical relationship between cortical areas manifesting contralateral (classical) retinotopy, compared with regions showing ipsilateral activity. Both patterns were produced and are displayed in the right hemisphere (subject LK). The ipsilateral activity (shown in red) was produced by the stimulus in Fig. 1A. The contralateral activity (yellow and blue) was produced by "thin" rings and rays, as described elsewhere (24). Regions showing significant contralateral retinotopy with polarity similar to that in the visual field are shown in yellow, and regions showing significant mirror-symmetric contralateral retinotopy are shown in blue. Other flattened format conventions are as described in accompanying figures.

along multiple dimensions, including color, motion, spatial configuration, and perhaps cognitive components.

The natural images were digitized from magazines, including landscapes and housing interiors, and presented in 8-bit color. The images were presented as stationary scenes, for 2 sec/presentation, in epochs 16 sec long, separated by epochs of uniform gray. Thus the stimulus timing and design was identical to that used for the moving gratings. Subjects were instructed to fixate the central point (as with the moving grating stimuli), but were given no additional instructions with regard to the naturalistic stimuli.

Fig. 5A shows the results of this type of ipsilateral stimulation, in comparison to ipsilateral stimulation with moving gratings in the same hemisphere (Fig. 5B). The activation produced by the naturalistic stimuli was located in similar regions of cortex (anterior to the areas showing contralateral retinotopy), compared with those activated by the moving gratings—thus our major conclusions about the location of ipsilateral activation were adequately supported.

However, finer details of the two activity patterns differ. In general, the activation produced by the naturalistic stimuli did not show the characteristic two-branched pattern produced by the moving gratings. Furthermore, the naturalistic activation extended more inferiorly in human cortex, further into the fusiform gyrus and other regions of the temporal lobe. Similar differences were obtained consistently in all subjects tested with these two stimuli. These results support our hypothesis that the correspondence between callosal and activity-driven maps actually may be slightly greater than was revealed in most of our tests, by using a single type of stimulus. Unfortunately, it is logically impossible to test the correspondence of the callosal maps to fMRI maps produced by all possible ipsilateral stimuli, and the available human callosal maps are likewise technically incomplete. Thus the degree of correspondence

between ipsilateral visual activity and callosal maps mediating this activity remains unresolved.

The relative expansion of the ipsilateral activity into the temporal lobe (when produced by the naturalistic stimuli) is consistent with the idea (from macaques) that color and form are processed more in a temporal "stream," whereas motion and spatial relations are processed more in a parietal "stream" (41–45). In human cortex, this idea has been supported in well-controlled experiments comparing attention to form vs. attention to spatial relations (46). The present experiments suggest that more direct tests of bilateral stimulus specificity for form/color vs. motion/spatial relations might also successfully differentiate temporal vs. parietal "streams."

Conclusions

The results presented here, and previous results using other techniques, suggest the following generalities. Human visual information is processed first in the contralateral visual field, then gradually it crosses the vertical meridian as receptive fields become larger and extend into the ipsilateral visual field. Visual information is represented even more bilaterally in correspondingly more anterior areas, with much larger receptive fields and without demonstrable retinotopy. Converging fMRI evidence suggests that human area MT and the lateral occipital region have such bilaterally responsive, large, poorly retinotopic receptive fields.

The extent of ipsilateral influence can change abruptly at the border between cortical areas, as between human areas V3A/V4v vs. V3/VP (see Fig. 4). Thus these maps of the ipsilateral retinotopy may help to differentiate human cortical areas invisible by other means.

These results also indicate that psychophysical comparisons of stimuli in the two visual field must avoid the vertical meridian by significantly more than 40° (polar angle) for maximum independence. Complete interhemispheric independence may be impossible to achieve throughout visual cortex.

The ipsilateral visual representation is thus a highly organized system, topographically well integrated with other aspects of the human visual cortical organization. The communication across the interhemispheric "seam" in higher visual areas presumably is related to the construction of a unitary visual percept, uniting the two hemifield maps present in lower-tier areas. Though we focus here on this interhemispheric seam in visual cortex, a similar approach (using different stimuli) should make it possible to map the interhemispheric seam in additional cortical systems.

We thank Mary Foley, Terrance Campbell, William Kennedy, Bruce Rosen, and Thomas Brady for invaluable assistance during the course of this project. We are grateful to Martin Sereno for significant comments on a previous version of this manuscript. This work was supported by grants from the Human Frontiers Science Program and National Eye Institute to R.B.H.T., the Swiss Fonds National de la Recherche Scientifique to N.K.H., and the McDonnell-Pew Foundation to J.D.M.

1. Dow, B. M., Snyder, A. Z., Vautin, R. G. & Bauer, R. (1981) *Exp. Brain Res.* **44**, 213–228.
2. Tootell, R. B. H., Siverman, M. S., Hamilton, S. L. & Switkes, E. (1988) *J. Neurosci.* **8**, 1531–1568.
3. Zeki, S. (1970) *Brain Res.* **19**, 63–75.
4. Van Essen, D. C. & Zeki, S. M. (1978) *J. Physiol. (London)* **277**, 193–226.
5. Newsome, W. T. & Allman, J. M. (1980) *J. Comp. Neurol.* **194**, 209–233.
6. Van Essen, D. C., Newsome, W. T. & Bixby, J. L. (1983) *J. Neurosci.* **2**, 265–283.
7. Cusick, C. G., Gould, H. J. & Kaas, J. H. (1984) *J. Comp. Neurol.* **230**, 311–336.
8. Beck, P. D. & Kaas, J. H. (1994) *Brain Res.* **651**, 57–75.

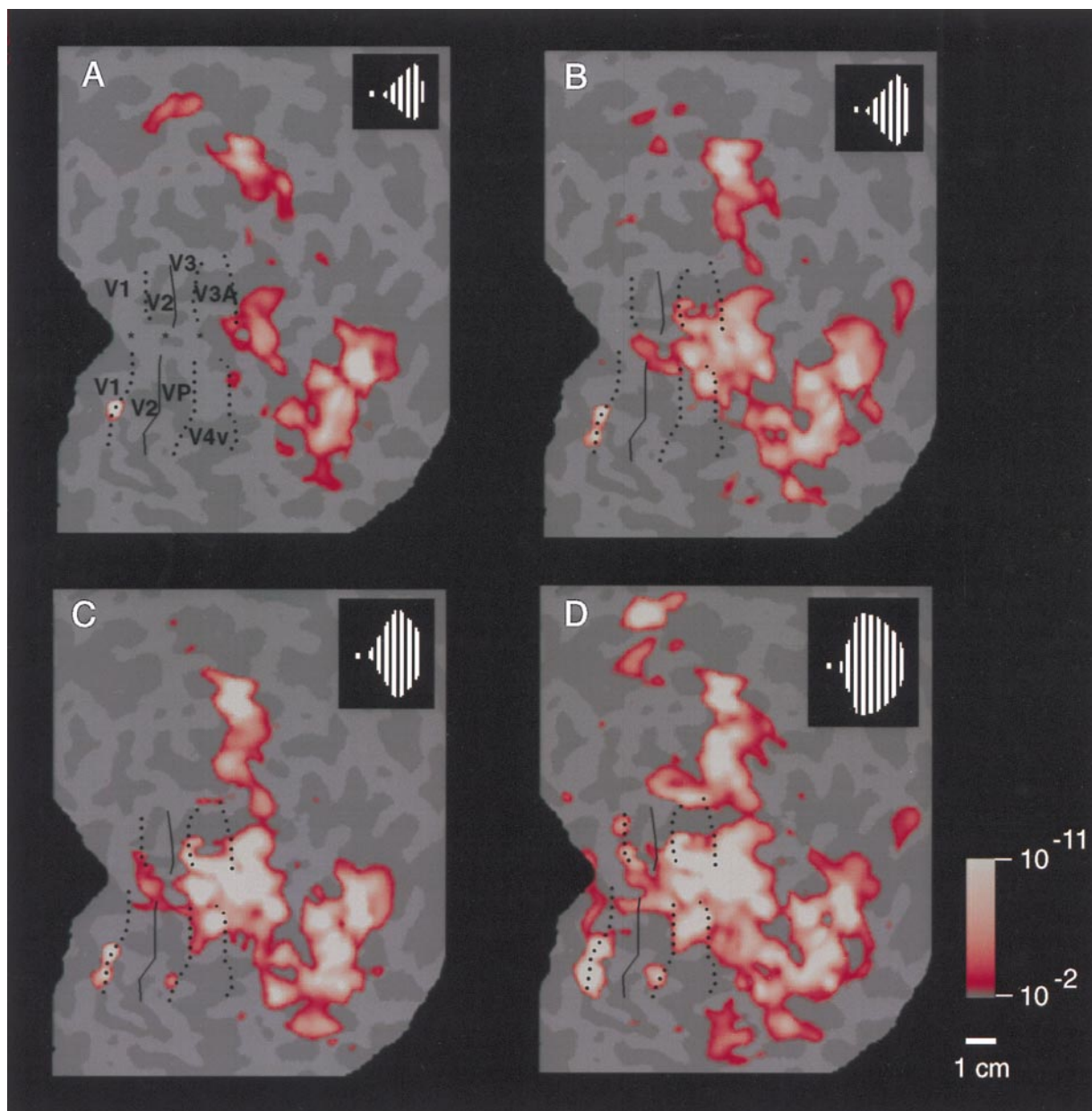


FIG. 4. Range of activity produced by stimuli of systematically varied extent in the ipsilateral visual field. Stimuli such as that in Fig. 1A were presented within a range of sector sizes (shown in Fig. 1B) in one representative ipsilateral hemisphere (subject JM). The stimulus was displaced from the vertical meridian by 40° of polar angle in A, 20° in B, 10° in C, and 5° in D (see logos). Visual cortical area borders, revealed in the same hemisphere by tests of contralateral retinotopy, are indicated for comparison. Representations of the contralateral horizontal meridian are indicated by solid lines, and representations of the vertical meridia are indicated by dashed lines. The pseudocolor activity scale bar is as described above, except that MR decreases are not shown, for simplicity. In general, cortical activity increased as the stimulus encroaches progressively closer to the vertical meridian. Within early retinotopic areas, such as the border between V1 and V2 (especially C and D), activity appeared first at the representation of the vertical meridian. Ipsilateral activity was correspondingly lacking at area borders corresponding to the contralateral horizontal meridian, such as the borders between V2/V3 and V2/VP. There were also distinct differences between areas in the degree of ipsilateral activation: across a significant range of stimulus extent ($5\text{--}20^\circ$ in this example), areas V3A and V4v showed more widespread ipsilateral activation than immediately adjacent areas V3 and VP. Furthermore, the activity in V3A and V4v extended well beyond the vertical meridian representations of these areas, even though these areas show clear contralateral retinotopy in other tests. The differences in ipsilateral fMRI topography between lower (e.g., V1, V2, and V3/VP) vs. presumably higher-tier (e.g., V3A and V4v) retinotopic areas is consistent with the presence of larger receptive fields in the latter. This evidence for larger receptive fields in V3A/V4v is also consistent with other human fMRI (24) and macaque electrophysiology (40).

9. Desimone, R. & Ungerleider, L. G. (1986) *J. Comp. Neurol.* **248**, 164–189.
10. Tanaka, K. & Saito, H. (1989) *J. Neurophysiol.* **62**, 626–641.
11. Duffy, C. J. & Wurtz, R. H. (1991) *J. Neurophysiol.* **65**, 1329–1345.
12. Raiguel, S., Van Hulle, M. M., Xiao, D. K., Marcar, V. L., Lagae, L. & Orban, G. A. (1997) *NeuroReport* **8**, 2803–2808.
13. Blatt, G. J., Andersen, R. A. & Stoner, G. R. (1990) *J. Comp. Neurol.* **299**, 421–445.
14. Desimone, R., Moran, J., Stein, S. J. & Mishkin, M. (1993) *Visual Neurosci.* **10**, 159–171.
15. Gross, C. G., Rocha-Miranda, C. E. & Bender, D. B. (1972) *J. Neurophysiol.* **35**, 96–111.
16. DeYoe, E. A., Felleman, D. J., Van Essen, D. C. & McClendon, E. (1994) *Nature (London)* **371**, 151–154.
17. Clarke, S. & Miklosy, J. (1990) *J. Comp. Neurol.* **298**, 188–214.
18. Hadjikhani, N., Clarke, S., Van Essen, D. C., Drury, H. & Kraftsik, R. (1994) *Eur. J. Neurosci.* **7**, Suppl., 189 (abstr.).

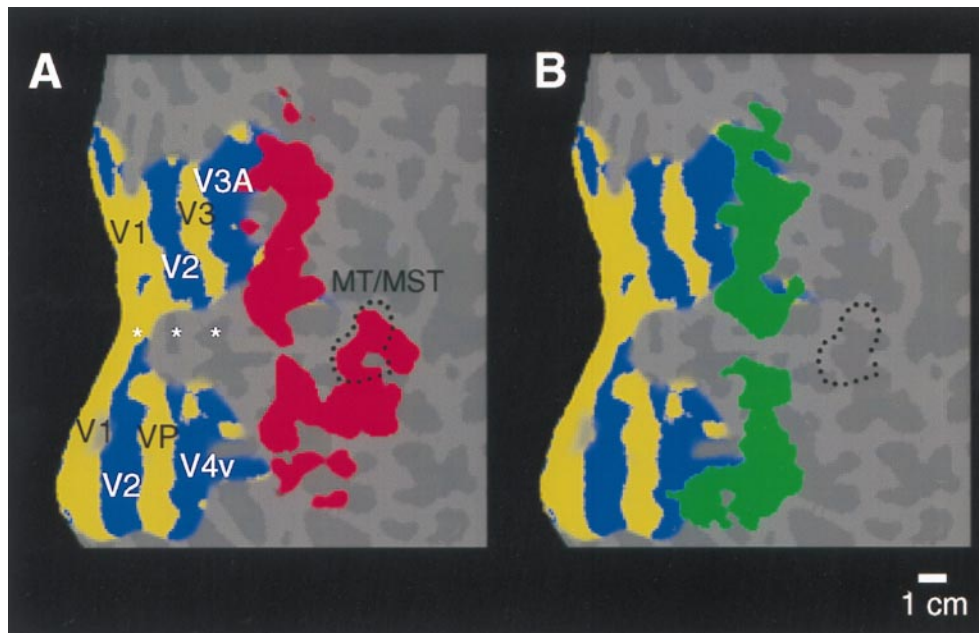


FIG. 5. Comparison of the ipsilateral activity produced by two different stimuli, within the same unilateral aperture. (A) The typical pattern of activation produced by the moving gratings, in the ipsilateral aperture shown in Fig. 1A (20° in polar angle from the vertical meridian). Significant ipsilateral activity is coded red, and the retinotopic field sign map from the same hemisphere is shown in yellow/blue. As described earlier, this stimulus produces a bifurcating pattern concentrated anterior to V3A/V4v, with the lower branch extending through MT. (B) Data from a similar experiment in the same hemisphere, with the same field sign map for comparison. In this second experiment, naturalistic images were presented within the same ipsilateral apertures, again avoiding the vertical meridian by 20° of polar angle. Activity in response to this stimulus is thresholded as in A and coded green. The upper branch of both ipsilateral activity patterns is similar. However, the lower branch of activity produced by the naturalistic stimuli does not extend anteriorly through MT. Instead it extends further inferior (downward in the figure), compared with that produced by the moving gratings in the same apertures. Similar differences were seen in all subjects tested with these two stimuli.

19. Van Essen, D. C., Clarke, S., Hadjikhani, N., Drury, H., Coogan, T., Carman, G. & Kraftsik, R. (1994) *Soc. Neurosci. Abstr.* **20**, 428.
20. Sperry, R. W. (1968) *Am. Psychol.* **23**, 723–733.
21. Sperry, R. W., Gazzaniga, M. S. & Bogen, J. E. (1979) in *Handbook of Clinical Neurology*, eds. Vinken, P. J. & Bruyn, G. W. (North-Holland, Amsterdam), pp. 273–290.
22. Kaas, J. H. (1995) *Curr. Biol.* **5**, 1126–1128.
23. Tootell, R. B. H., Dale, A. M., Sereno, M. I. & Malach, R. (1966) *Trends Neurosci.* **19**, 481–489.
24. Tootell, R. B. H., Mendola, J. D., Hadjikhani, N. K., Ledden, P. A., Liu, A. K., Reppas, J. B., Sereno, M. I. & Dale, A. M. (1997) *J. Neurosci.* **17**, 7060–7078.
25. Schneider, W., Noll, D. C. & Cohen, J. D. (1993) *Nature (London)* **365**, 150–153.
26. Engel, S. A., Rumelhart, D. E., Wandell, B. A., Lee, A. T., Glover, G. H., Chichilnisky, E. J. & Shadlen, M. N. (1994) *Nature (London)* **370**, 106.
27. DeYoe, E. A., Bandettini, P., Neitz, J., Miller, D. & Winans, P. (1994) *J. Neurosci. Methods* **54**, 171–187.
28. Tootell, R. B. H., Reppas, J. B., Kwong, K. K., Malach, R., Born, R. T., Brady, T. J., Rosen, B. R. & Belliveau, J. W. (1995) *J. Neurosci.* **15**, 3215–3230.
29. Sereno, M. I., Dale, A. M., Reppas, J. B., Kwong, K. K., Belliveau, J. W., Brady, T. J., Rosen, B. R. & Tootell, R. B. H. (1995) *Science* **268**, 889–893.
30. DeYoe, E. A., Carman, G. J., Bandettini, P., Glickman, S., Wieser, J., Cox, R., Miller, D. & Neitz, J. (1996) *Proc. Natl. Acad. Sci. USA* **93**, 2382–2386.
31. Engel, S. A., Glover, G. H. & Wandell, B. A. (1997) *Cereb. Cortex* **7**, 181–192.
32. Lueck, C. J., Zeki, S., Friston, K. J., Dieber, M.-P., Cope, P., Cunningham, V. J., Lammertsma, A. A., Kennard, C. & Frackowiak, R. S. J. (1989) *Nature (London)* **340**, 386–389.
33. Zeki, S., Watson, J. D. G., Lueck, C. J., Friston, K. J., Kennard, C. & Frackowiak, R. S. J. (1991) *J. Neurosci.* **11**, 641–649.
34. Watson, J. D. G., Myers, R., Frackowiak, R. S. J., Hajnal, J. V., Woods, R. P., Mazziota, J. C., Shipp, S. & Zeki S. (1993) *Cereb. Cortex* **3**, 79–94.
35. Tootell, R. B. H., Reppas, J. B., Dale, A. D., Look, R. B., Malach, R., Jiang, H.-J., Brady, T. J. & Rosen, B. R. (1995) *Nature (London)* **375**, 139–141.
36. McCarthy, G., Spicer, M., Adrignolo, A., Luby, M., Gore, J. & Allison, T. (1995) *Hum. Brain Mapp.* **2**, 234–243.
37. Dale, A. M. & Sereno, M. I. (1993) *J. Cognit. Neurosci.* **5**, 162–176.
38. Drury, H. A., Van Essen, D. C., Anderson, C. H., Lee, C. W., Coogan, T. A. & Lewis, J. W. (1996) *J. Cognit. Neurosci.* **8**, 1–28.
39. Felleman, D. J. & Van Essen, D. C. (1991) *Cereb. Cortex* **1**, 1–47.
40. Gattas, R., Sousa, A. P. B. & Covey, E. (1985) in *Pattern Recognition Mechanisms*, eds. Chagas, R., Gattas, R. & Gross, C. (Pontificae Academiae Scientiarum Scripta Varia, Rome), Vol. 54, pp. 1–20.
41. Ungerleider, L. G. & Mishkin, M. (1982) in *Analysis of Visual Behavior*, eds. Ingle, D. J., Goodale, M. A. & Mansfield, R. J. W. (MIT Press, Cambridge, MA), pp. 549–586.
42. Maunsell, J. H. R. (1987) in *Matters of Intelligence*, ed. Vaina, L. (Reidel, Dordrecht, The Netherlands), pp. 59–87.
43. DeYoe, E. A. & Van Essen, D. C. (1988) *Trends Neurosci.* **11**, 219–226.
44. Livingstone, M. & Hubel, D. H. (1988) *Science* **240**, 740–749.
45. Zeki, S. & Shipp, S. (1988) *Nature (London)* **335**, 311–317.
46. Haxby, J. V., Grady, C. L., Horowitz, B., Ungerleider, L. G., Mishkin, M., Carson, R. E., Herscovitch, P., Schapiro, M. B. & Rapoport, S. I. (1991) *Proc. Natl. Acad. Sci. USA* **88**, 1621–1625.